Electronic Supplementary Material (ESI) for CrystEngComm.

Supporting Information

Pharmaceutical nanococrystal synthesis: a novel grinding approach

João A. V. Santos,[a] João A. Baptista,[a] Inês C. Santos, [a] Teresa M. R. Maria, [a] João Canotilho, [a,b] Ricardo A. E. Castro*,[a,b] M. Ermelinda S. Eusébio*,[a]

[a]CQC, Departamento de Química, Universidade de Coimbra, Portugal

E-mail: quierme@ci.uc.pt

[b]Faculdade de Farmácia, Universidade de Coimbra, Portugal

E-mail: rcastro@ff.uc.pt

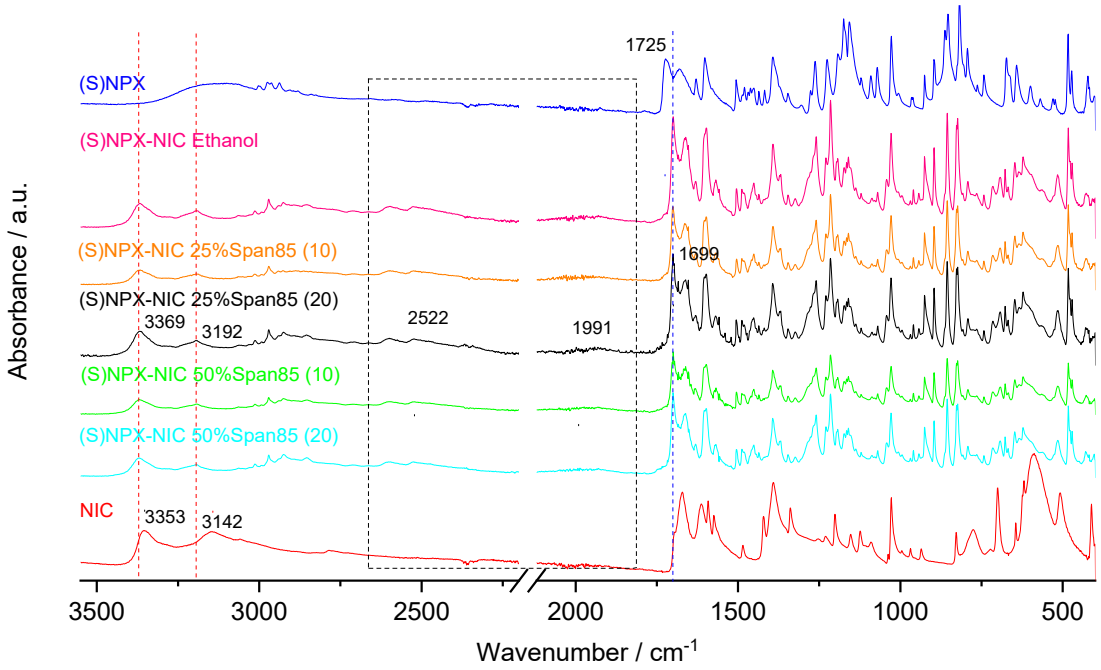

Figure S1: IR spectra of (2:1) (S)NPX-NIC cocrystals, synthesized by SAG, in the presence of Span® 85, and comparison with the cocrystal obtained by ethanol assisted grinding and with initial solids: --- deviation of NH_2 asymmetric and symmetric stretching bands; --- deviation of C=O stretching band; --- new bands corresponding to the formation of hydrogen bonds, $COOH...N_{aromatic}$.

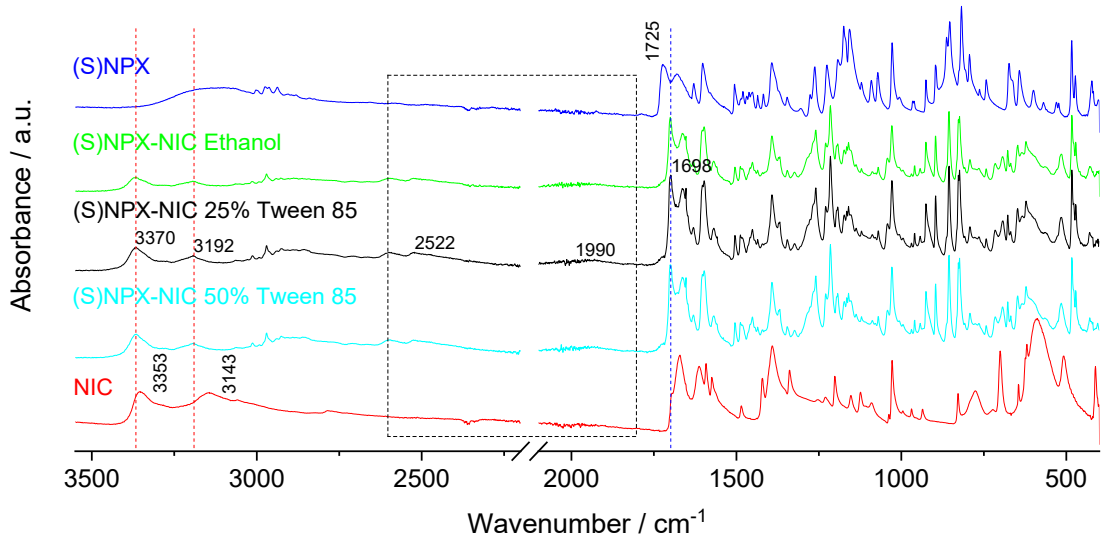

Figure S2: IR spectra of (2:1) (S)NPX-NIC cocrystals, synthesized by SAG, in the presence of Tween® 85, and comparison with the cocrystal obtained by ethanol assisted grinding and with initial solids: --- deviation of NH_2 asymmetric and symmetric stretching bands; --- deviation of stretching C=O band; --- new bands corresponding to the formation of hydrogen bonds, COOH...$N_{aromatic}$.

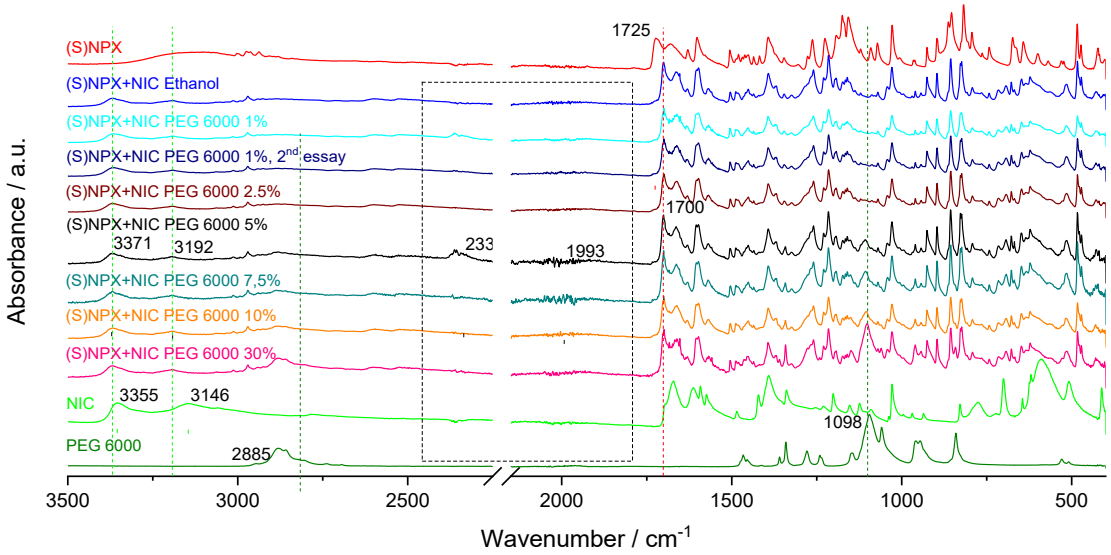

Figure S3: IR spectra of (2:1) (S)NPX-NIC cocrystals, synthesized by POLAG, in the presence of PEG 6000, and comparison with the cocrystal obtained by ethanol assisted grinding and with initial solids: --- deviation of NH_2 asymmetric and symmetric stretching bands; --- deviation of stretching C=O band; --- new bands corresponding to the formation of hydrogen bonds, COOH...$N_{aromatic}$; --- bands from PEG 6000 that can be observed on the samples with the increase of polymer mass %.

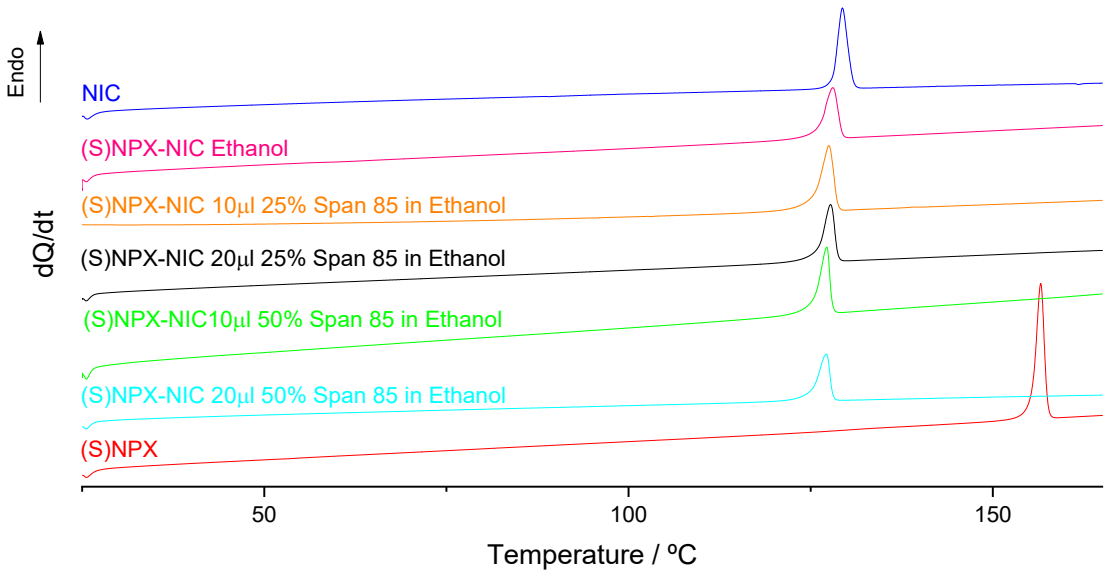

Figure S4: Comparison between DSC heating curves of (2:1) (S)NPX-NIC cocrystals obtained by SAG, in the presence of Span® 85, the starting solids and the cocrystal obtained by ethanol assisted grinding.

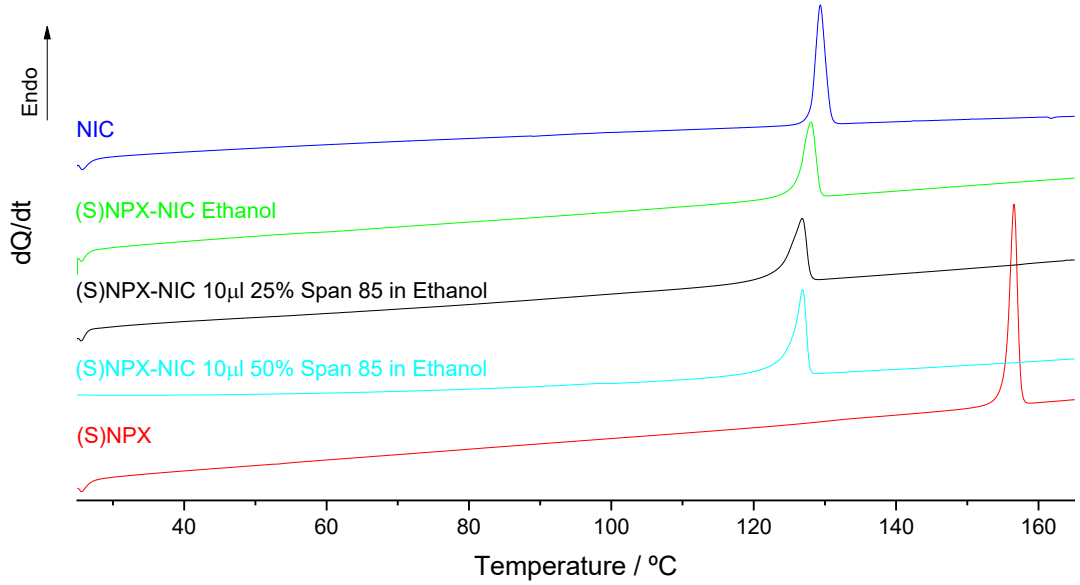

Figure S5: Comparison between DSC heating curves of (2:1) (S)NPX-NIC cocrystals obtained by SAG, in the presence of Tween® 85, the starting solids and the cocrystal obtained by ethanol assisted grinding.

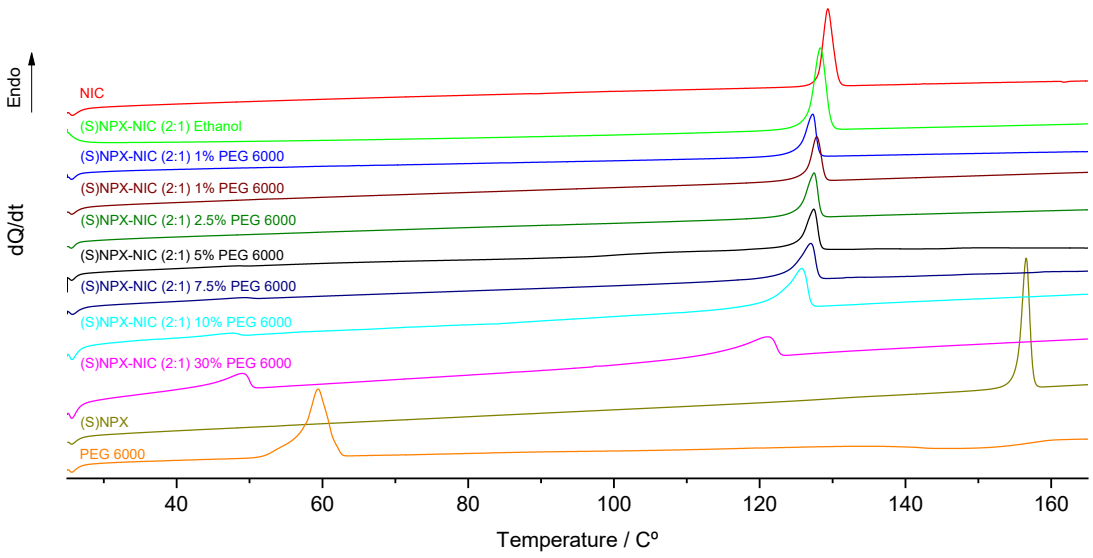

Figure S6: Comparison between DSC heating curves of (2:1) (S)NPX-NIC cocrystals obtained by POLAG, in the presence of PEG 6000, the starting solids and the cocrystal obtained by ethanol assisted grinding.

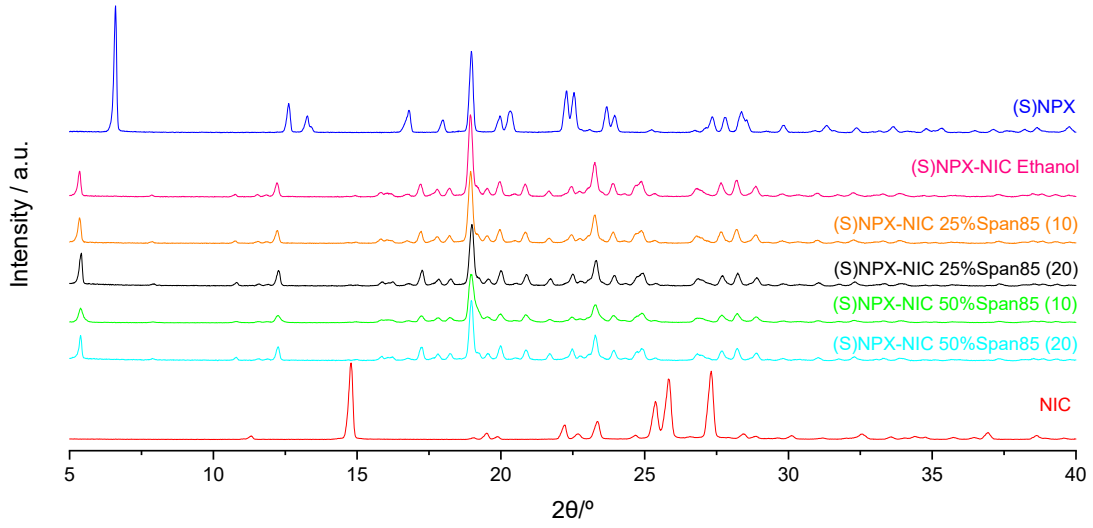

Figure S7: Comparison between XRPD diffractograms of (2:1) (S)NPX-NIC cocrystals obtained by SAG, in the presence of Span® 85, the starting solids and the cocrystal obtained by ethanol assisted grinding.

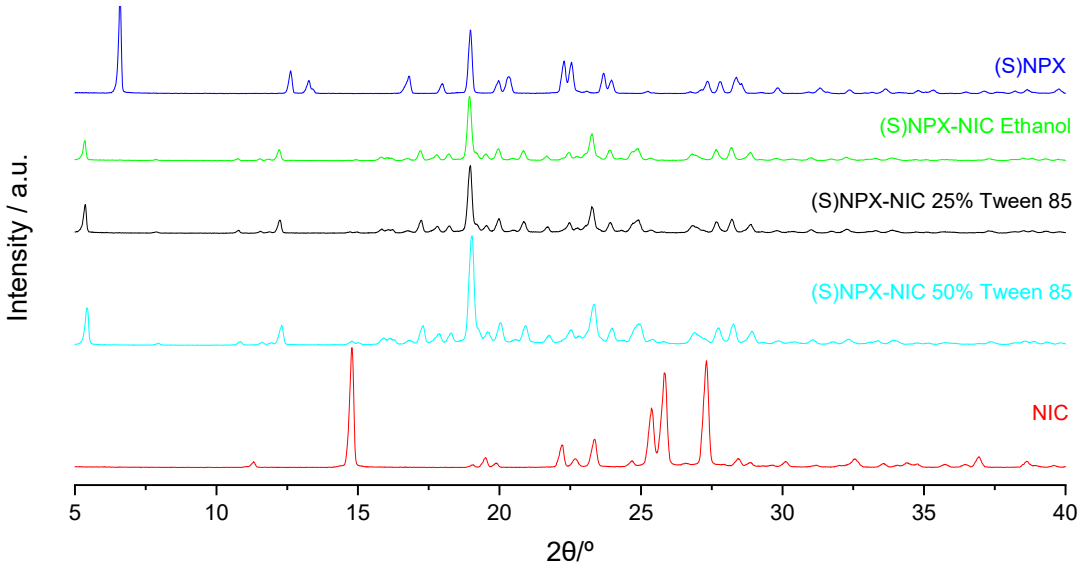

Figure S8: Comparison between XRPD diffractograms of (2:1) (S)NPX-NIC cocrystals obtained by SAG, in the presence of Tween® 85, the starting solids and the cocrystal obtained by ethanol assisted grinding.

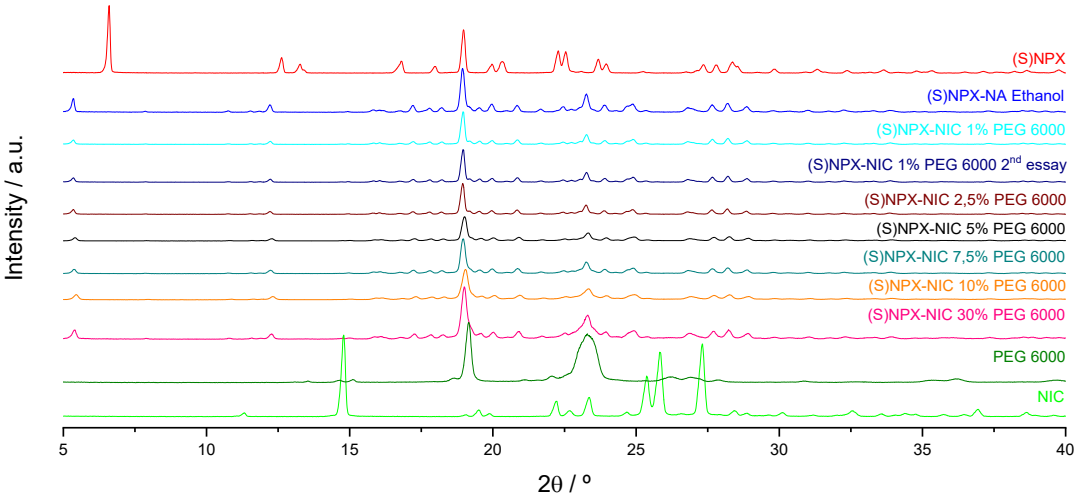

Figure S9: Comparison between XRPD diffractograms of (2:1) (S)NPX-NIC cocrystals obtained by POLAG, in the presence of PEG 6000, the starting solids and the cocrystal obtained by ethanol assisted grinding.

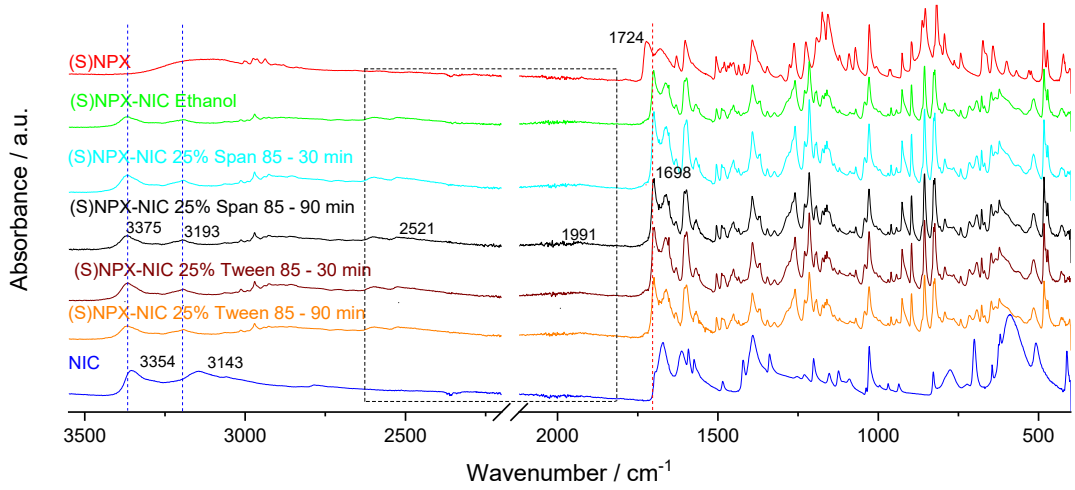

Figure S10: IR spectra of (2:1) (S)NPX-NIC cocrystals, synthesized by SAG, in the presence of Span® 85 or Tween® 85, grinded during 30 and 90 min, comparison with the cocrystal obtained by ethanol assisted grinding and with the initial solids: --- deviation of NH_2 asymmetric and symmetric stretching bands; --- deviation of stretching C=O band; --- new bands corresponding to the formation of hydrogen bonds, $COOH...N_{aromatic}$.

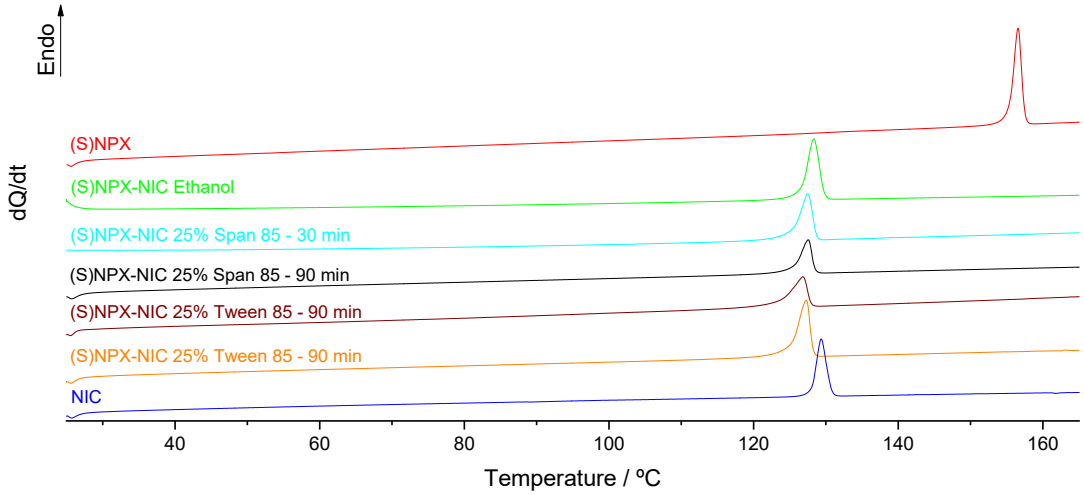

Figure S11: DSC heating curves of (2:1) (S)NPX-NIC cocrystals obtained by SAG in the presence of Span® 85 or Tween® 85, grinded with different milling times; comparison with the starting solids and with the cocrystal obtained by ethanol assisted grinding.

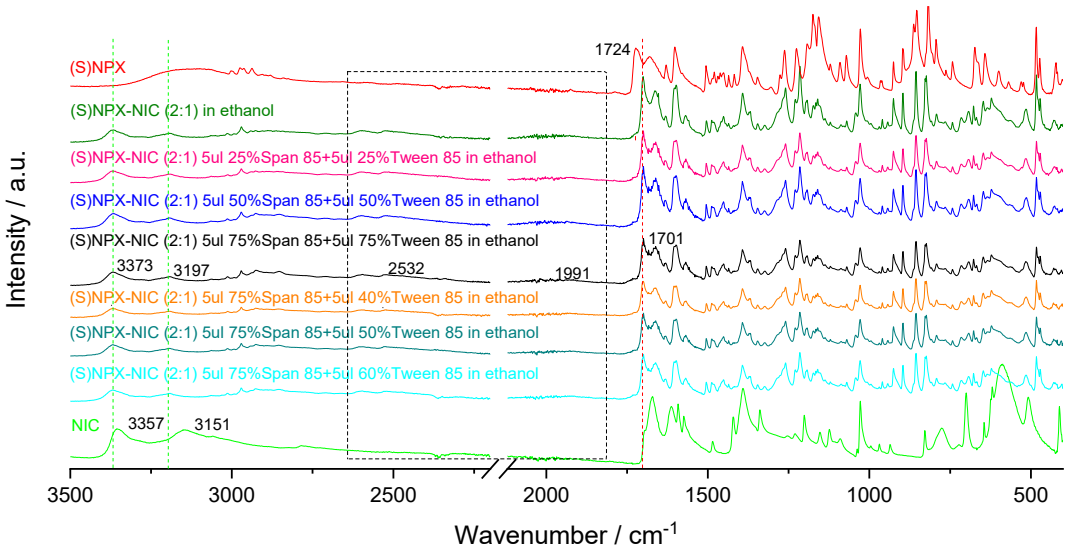

Figure S12: IR spectra of (2:1) (S)NPX-NIC cocrystals, synthesized by SAG, in the presence of mixtures of Span® 85 and Tween® 85, in different percentages, and comparison with the cocrystal obtained by ethanol assisted grinding and with thestarting solids: --- deviation of NH_2 asymmetric and symmetric stretching bands; --- deviation of stretching C=O band; --- new bands corresponding to the formation of hydrogen bonds, COOH...$N_{aromatic}$.

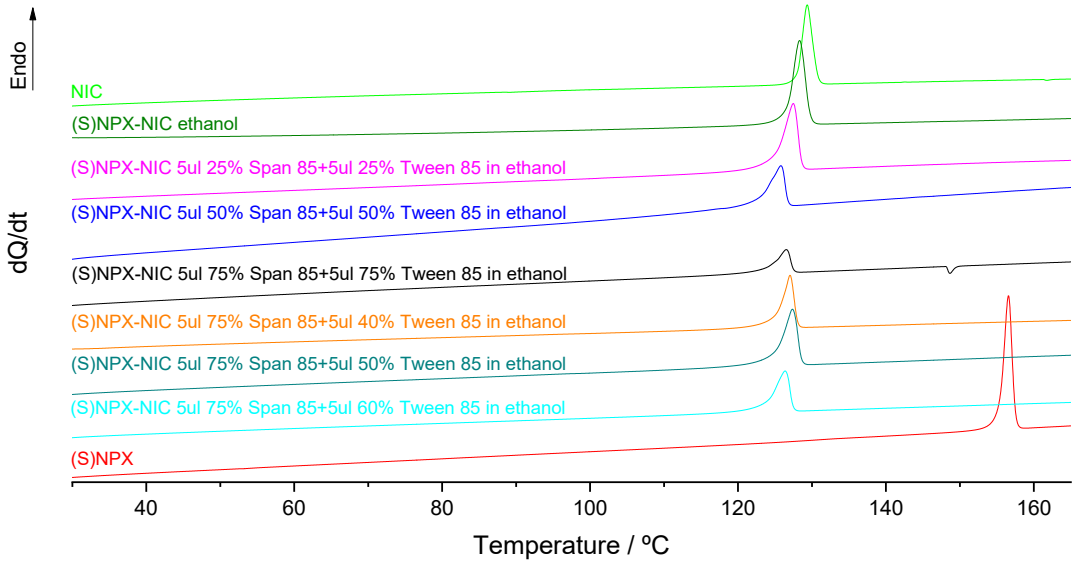

Figure S13: Comparison between DSC heating curves of (2:1) (S)NPX-NIC cocrystals obtained by SAG assisted with ethanolic mixtures of the combined surfactants, the starting solids and the cocrystal obtained by ethanol assisted grinding. The surfactant mixtures are composed by Span® 85 and Tween® 85 in different volume percentages on the ethanolic mixture (% V/V).

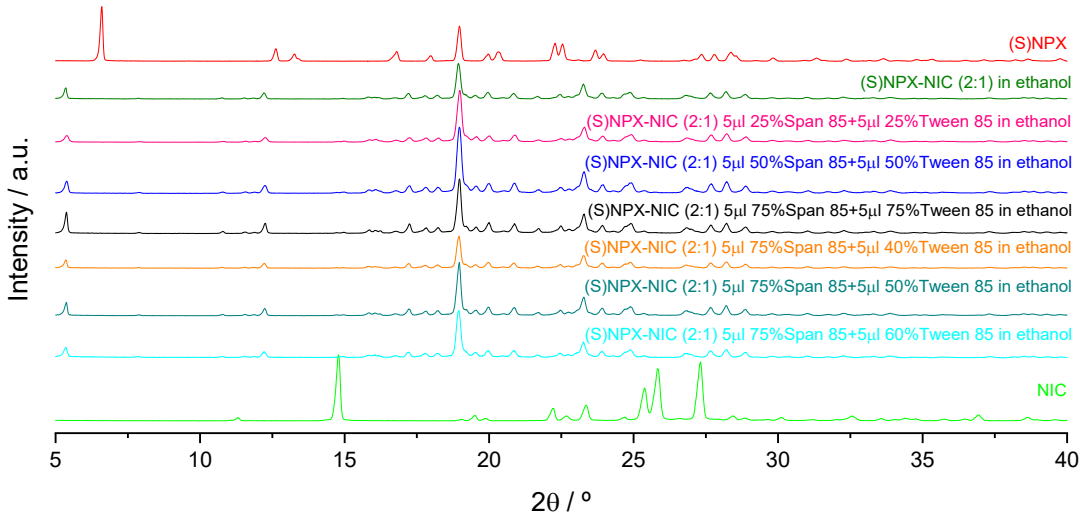

Figure S14: Comparison between XRPD diffractograms of (2:1) (S)NPX-NIC cocrystals obtained by SAG, in the presence of mixtures of Span® 85 and Tween® 85 in different percentages of the total volume of the ethanolic mixture, the starting solids and the cocrystal obtained by ethanol assisted grinding.

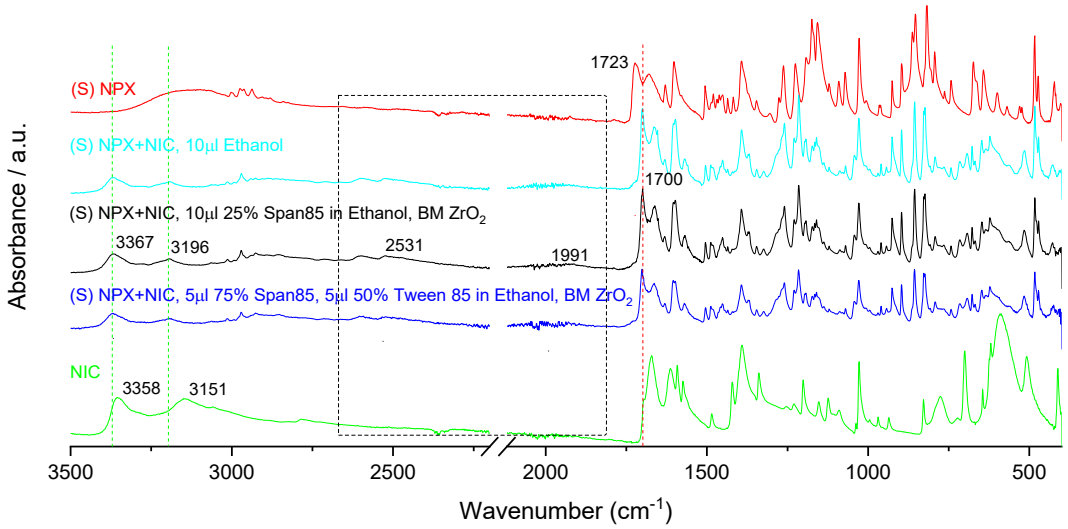

Figure S15: IR spectra of (2:1) (S)NPX-NIC cocrystals, synthesized by SAG, in the presence of an ethanolic mixture of Span® 85 and of an optimized ethanolic mixture of Span® 85 and Tween® 85, grinded in zirconium oxide vessels (BM ZrO_2): --- deviation of NH_2 asymmetric and symmetric stretching bands; --- deviation of stretching C=O band; --- new bands corresponding to the formation of hydrogen bonds, COOH...$N_{aromatic}$. The spectra of the obtained cocrystal is compared with the ones of the starting solids and the cocrystal obtained by LAG assisted with ethanol.

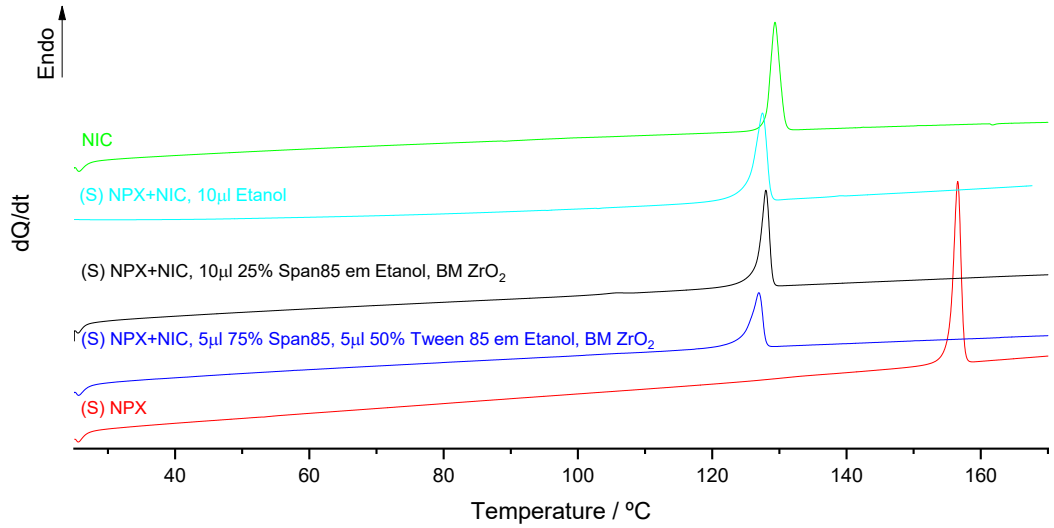

Figure S 16: DSC heating curves of (2:1) (S)NPX-NIC cocrystals obtained by SAG, assisted with an ethanolic mixture of the optimized surfactant combination, using zirconium oxide vessels (BM ZrO_2); comparison with the starting solids and with the and the cocrystal obtained by ethanol assisted grinding.

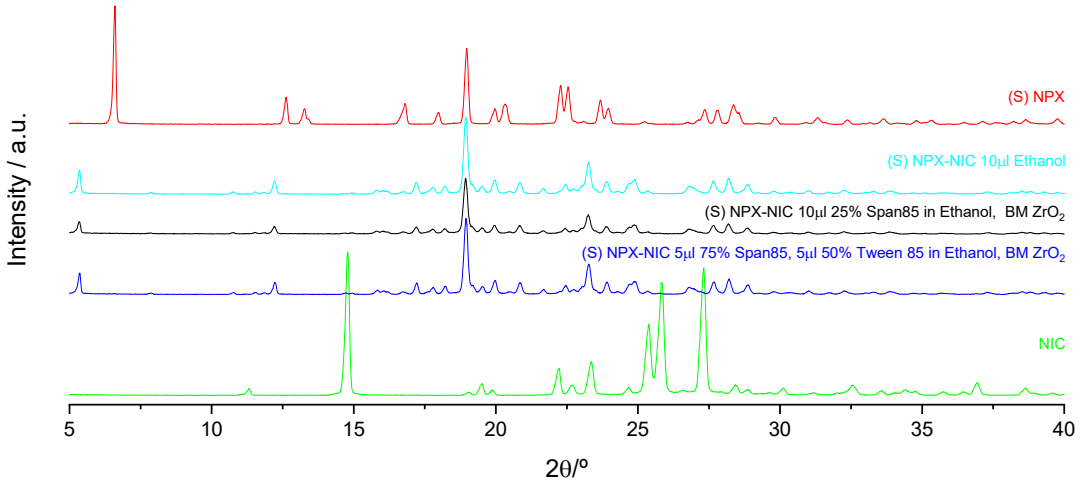

Figure S17: Comparison between XRPD diffractograms of (2:1) (S)NPX-NIC cocrystals obtained by SAG assisted with ethanolic mixtures of the optimized surfactant combination, using zirconium oxide vessels (BM ZrO_2), the starting solids and the cocrystal obtained by ethanol assisted grinding.

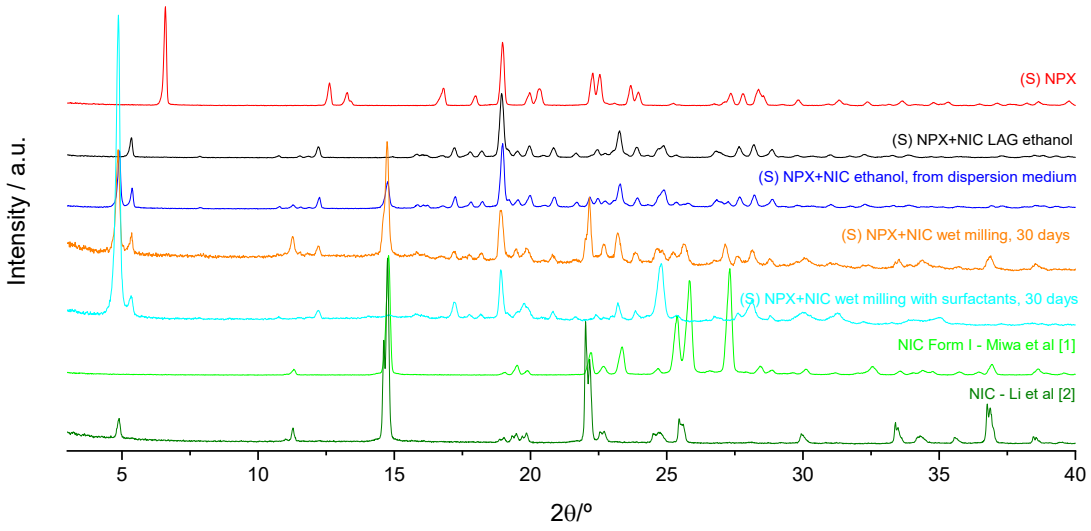

Figure S18: Comparison between XRPD diffractograms of dry (2:1) (S)NPX-NIC cocrystals obtained by ethanol assisted LAG (black) and the same cocrystals after being dispersed in the chosen medium (blue) revealing cocrystal stability in the used dispersion medium. In this later diffractogram (blue), nicotinamide reflections are also observed resulting from solvent evaporation, and consequent NIC crystallization, once it is present in higher concentration when compared to (S)NPX (red) in the dispersion medium. The cocrystal is also stable in the used dispersion medium 30 days after wet milling application, with (cyan) and without surfactants (orange), again with the diffractograms representing a sum of that of the cocrystal with the those of NIC polymorphs.

Table S1: Thermodynamic parameters obtained from the DSC heating curves of (2:1) (S)NPX-NIC systems, prepared by SAG, stabilized with Span® 85. Comparison with the starting and solids and with the cocrystal obtained by ethanol assisted grinding.

	T_{fus} / °C ($\Delta_{fus}H$ / kJ mol^{-1})	
	Experimental	**Literature**
NIC	128.1 (23.2)[a)]	128.2 ± 0.2 (23.2 ± 0.4)[a?]
(S)NPX-NIC Ethanol	126.1 (74.6)[a)]	125.6 ± 0.4 (75.0 ± 1.0)[a)]
(S)NPX-NIC 10 µl 25% Span 85 in Ethanol	125.2	-
(S)NPX-NIC 20 µl 25% Span 85 in Ethanol	125.9	-
(S)NPX-NIC 10 µl 50% Span 85 in Ethanol	125.3	-
(S)NPX-NIC 20 µl 50% Span 85 in Ethanol	125.1	-
(S)NPX	155.3 (32.7)[a)]	155.6 ± 0.2 (33.0 ± 0.5)[a)]

a) Values from literature.[3]

Table S2: Thermodynamic parameters obtained from the DSC heating curves of (2:1) (S)NPX-NIC systems, prepared by SAG, stabilized with Tween® 85. Comparison with the starting solids and with the cocrystal obtained by ethanol

	T_{fus} / °C ($\Delta_{fus}H$ / kJ mol^{-1})	
	Experimental	**Literature**
NIC	128.1 (23.2)[a)]	128.2 ± 0.2 (23.2 ± 0.4)[a)]
(S)NPX-NIC Etanol	126.1 (74.6)[a)]	125.6 ± 0.4 (75.0 ± 1.0)[a)]
(S)NPX-NIC 10 µl 25% Tween® 85 in Ethanol	123.6	-
(S)NPX-NIC 10 µl 50% Tween® 85 in Ethanol	124.9	-
(S)NPX	155.3 (32.7)[a)]	155.6 ± 0.2 (33.0 ± 0.5)[a)]

assisted grinding.

a) Values from literature.[3]

Table S3: Thermodynamic parameters of (S)NPX-NIC systems, stabilized with PEG 6000. Comparison with the starting solids and the stabilizer parameters.

	T_{fus} / °C ($\Delta_{fus}H$ / kJ mol^{-1})	
	Experimental	**Literature**
NIC	128.1 (23.2)[a]	128.2 ± 0.2 (23.2 ± 0.4)[a)]
(S)NPX-NIC Etanol	126.1 (74.6)[a)]	125.6 ± 0.4 (75.0 ± 1.0)[a)]
(S)NPX-NIC 1.0 % PEG 6000	125.3	-
(S)NPX-NIC 1.0 % PEG 6000	126.3	-
(S)NPX-NIC 2.5 % PEG 6000	125.3	-
(S)NPX-NIC 5.0 % PEG 6000	125.3	-
(S)NPX-NIC 7.5 % PEG 6000	123.8	-
(S)NPX-NIC 10.0 % PEG 6000	122.0	-
(S)NPX-NIC 30.0 % PEG 6000	113.3	-
(S)NPX	155.3 (32.7)[a)]	155.6 ± 0.2 (33.0 ± 0.5)[a)]
PEG 6000	56.7 (1116)	57.0 (1994)[b),c)]

a) Values from literature.[3]
b) Values from literature.[4]
c) Values from literature.[5]

Table S4: Comparison between thermodynamic parameters of (S)NPX-NIC systems obtained with grinding times of 30 and 90 min, and the starting solids.

	T_{fus} / °C ($\Delta_{fus}H$ / kJ mol^{-1})	
	Experimental	**Literature**
(S)NPX	155.3 (32.7)[a)]	155.6 ± 0.2 (33.0 ± 0.5)[a)]
(S)NPX-NIC Ethanol	126.1 (74.6)[a)]	125.6 ± 0.4 (75.0 ± 1.0)[a)]
(S)NPX-NIC 10 µl 25% Span® 85, 30 min	125.2	-
(S)NPX-NIC 10 µl 25% Tween® 85, 30 min	123.6	-
(S)NPX-NIC 10 µl 25% Span® 85, 90 min	125.5	-
(S)NPX-NIC 10 µl 25% Tween® 85, 90 min	125.1	-
NIC	128.1 (23.2)[a]	128.2 ± 0.2 (23.2 ± 0.4)[a)]

a) Values from literature.[3]

Table S5: Comparison between thermodynamic parameters of (S)NPX-NIC systems obtained with grinding assisted by different mixtures of Span® 85 and Tween® 85 in ethanol, and the starting solids.

	T_{fus} / °C ($\Delta_{fus}H$ / kJ mol^{-1})	
	Experimental	**Literature**
(S)NPX	155.3 (32.7)[a)]	155.6 ± 0.2 (33.0 ± 0.5)[a)]
(S)NPX-NIC Etanol	126.1 (74.6)[a)]	125.6 ± 0.4 (75.0 ± 1.0)[a)]
(S)NPX-NIC 5 µl 25% Span 85 + 5 µl 25% Tween 85	124.8	-
(S)NPX-NIC 5 µl 50% Span 85 + 5 µl 50% Tween 85	122.7	-
(S)NPX-NIC 5 µl 75% Span 85 + 5 µl 75% Tween 85	124.1	-
(S)NPX-NIC 5 µl 75% Span 85 + 5 µl 40% Tween 85	125.2	-
(S)NPX-NIC 5 µl 75% Span 85 + 5 µl 50% Tween 85	124.9	-
(S)NPX-NIC 5 µl 25% Span 85 + 5 µl 60% Tween 85	123.7	-
NIC	128.1 (23.2)[a]	128.2 ± 0.2 (23.2 ± 0.4)[a)]

a) Values from literature.[3]

Table S6: Comparison between thermodynamic parameters of (S)NPX-NIC systems obtained by SAG, using zirconium oxide vessels.

	T_{fus} / °C ($\Delta_{fus}H$ / kJ mol^{-1})	
	Experimental	**Literature**
(S)NPX	155.3 (32.7)[a)]	155.6 ± 0.2 (33.0 ± 0.5)[a)]
(S)NPX-NIC Etanol	126.1 (74.6)[a)]	125.6 ± 0.4 (75.0 ± 1.0)[a)]
(S)NPX-NIC 10 µl 25% Span 85 – ZrO_2	126.6	-
(S)NPX-NIC 5 µl 75% Span 85 + 5 µl 50% Tween 85 – ZrO_2	124.9	-
NIC	128.1 (23.2)[a]	128.2 ± 0.2 (23.2 ± 0.4)[a)]

a)Values from literature.[3]

References

1. Miwa Y., Mizuno T., Tsuchida K., Taga T.,Iwata Y., Experimental charge density and electrostatic potential in nicotinamide. Acta Crystallographica Section B-Structural Science, 1999; 55: 78-84.
2. Li X, Ou X, Wang B, Rong H, Wang B, Chang C, et al. Rich polymorphism in nicotinamide revealed by melt crystallization and crystal structure prediction. Communications Chemistry. 2020;3(1):152.
3. Castro RAE, Ribeiro JDB, Maria TMR, Ramos Silva M, Yuste-Vivas C, Canotilho J, et al. Naproxen Cocrystals with Pyridinecarboxamide Isomers. Crystal Growth & Design. 2011; 11: 5396-404.
4. Wang X, Michoel A, Van den Mooter G. Study of the phase behavior of polyethylene glycol 6000–itraconazole solid dispersions using DSC. International Journal of Pharmaceutics. 2004; 272: 181-7.
5. Clavaguera N, Saurina J, Lheritier J, Masse J, Chauvet A, Clavaguera-Mora MT. Eutectic mixtures for pharmaceutical applications: A thermodynamic and kinetic study. Thermochimica Acta. 1997; 290: 173-80.